

Polydopamine Modified by Pillar[5]arene In-situ for Targeted Chemo-Photothermal Cancer Therapy

Ruowen Tang, Lei Zhou, Yu Dai, Yang Wang,* Yan Cai, Tingting Chen, and Yong Yao*

School of Chemistry and Chemical Engineering, Nantong City Key Laboratory of Life-Organic Chemistry, Nantong University, Nantong, Jiangsu, 226019, P.R. China. E-mail: ywang85@ntu.edu.cn; yaoyong1986@ntu.edu.cn.

Supporting Information (19 pages)

1	Materials and methods	S2
2	Synthesis of P[5]OH	S4
3	Construction of PDA-P[5]OH nanoparticles	S9
4	Characterization	S10
5	Host-guest interaction	S11
6	In vivo study	S14

1. Materials and methods

Materials

All reagents were commercially available and used as supplied without further purification. Solvents were either employed as purchased or dried according to procedures described in the literature.

Measurements

NMR spectroscopy. ^1H and ^{13}C NMR spectra were recorded on a Bruker AV400 spectrometer.

UV/Vis spectroscopy. UV/Vis spectra and the optical transmittance were recorded in a quartz cell (light path 10 mm) on a Shimadzu UV-3600 spectrophotometer equipped with a PTC-348WI temperature controller.

ESI-MS spectroscopy. Electrospray ionization mass spectra (ESI-MS) were measured by Agilent 6520 Q-TOF-MS.

Cytotoxicity experiments. HeLa cells were incubated in Dulbecco's modified Eagle's medium (DMEM). The medium was supplemented with 10% fetal bovine serum and 1% Penicillin-Streptomycin. Cells were seeded in 96-well plates (5×10^4 cell mL^{-1} , 0.1 mL per well) for 4 h at 37°C in 5% CO_2 . Then the cells were incubated with different groups for 4 h. The relative cellular viability was determined by the MTT assay.

Fluorescence images. Cells were seeded in 6-well plates (5×10^4 cell mL^{-1} , 2 mL per well) for 24 h at 37°C in 5% CO_2 . The cells were incubated with the corresponding solution for 4 h. Then the medium was removed, and the cells were washed with phosphate buffer solution for three time. Finally, the cells were subjected to observation by a fluorescence microscope.

DLS spectroscopy. Solution samples were examined on a laser light scattering spectrometer (BI-200SM) equipped with a digital correlator (TurboCorr) at 636 nm at a scattering angle of 90°. The hydrodynamic diameter (Dh) was determined by DLS experiments at 25°C.

SEM. Scanning electron microscopy (SEM) investigations were carried out on a HitachiS-3400 SEM instrument.

TEM. The TEM images were obtained using a JEM-1200EX instrument with an accelerating voltage of 80 kV.

HPLC. The release of DOX was tracked by HPLC using a LC-20A High performance liquid chromatograph instrument (Shimadzu).

TGA. Thermal gravimetric analysis (TGA) was recorded on a PerkinElmer Pyris 1 instrument.

Flow cytometry.

The cell internalization of **PDA-P[5]OH@DOX**, **PDA-P[5]OH-FA-Py@DOX** and **PDA-P[5]OH-FA-Py@DOX + Folate (FA)** was investigated by Fluorescence images and flow cytometry. HeLa cells was seeded into 6-well tissue culture plate at a density of 5.0×10^5 cells/well and incubated for 24 h. Next, the fresh medium containing **PDA-P[5]OH@DOX**, **PDA-P[5]OH-FA-Py@DOX** and **PDA-P[5]OH-FA-Py@DOX + FA** with same drug concentration (5 $\mu\text{g}/\text{mL}$ DOX equiv.) was added to each well for selected time. Then, the medium containing drugs was removed, and the cells were washed with PBS, digested with trypsin, collected to analyze by flow cytometry.

In vivo studies

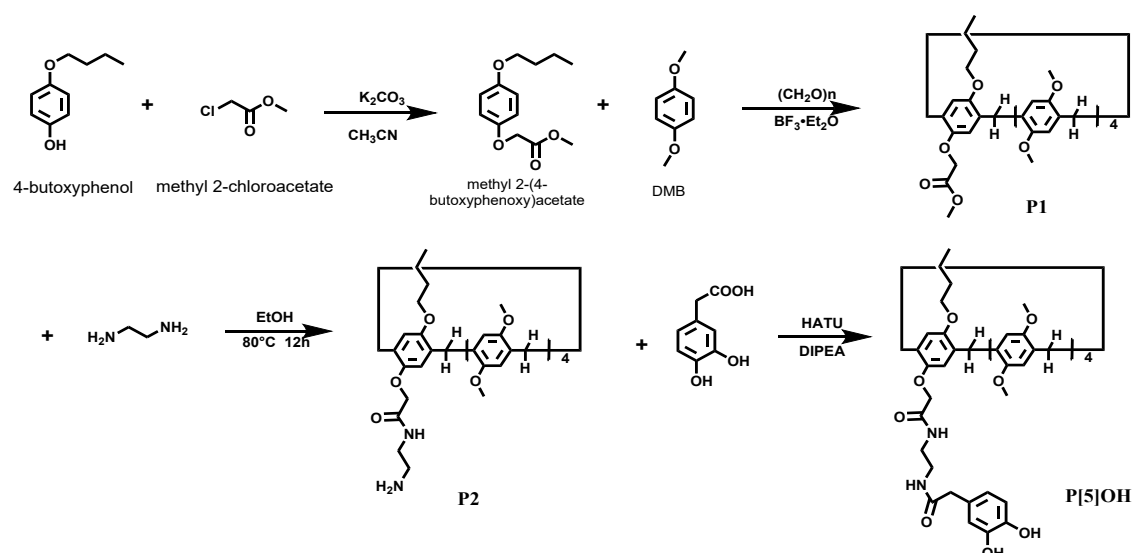
All animal procedures were conducted in compliance with the Nantong University Guidelines for Care and Use of Laboratory Animals and with the approval of the Nantong University Animal Ethics Committee.

Female nudist mice (4-6 weeks old, ~20 g) were housed under standard settings with 12 h light and dark cycles and had free access to food and water. The HeLa xenograft tumor model was utilized to investigate the treatment efficacy as an example. To achieve this, 100 μL 1×10^7 HeLa cells were injected subcutaneously into the rear of each mouse. The mice were randomly separated into six groups ($n = 3$) when the size of the tumor on the right hind back reached $\sim 100 \text{ mm}^3$. Then intravenously injected at 0 day with **PDA-P[5]OH**, **PDA-P[5]OH-FA-Py**, **Control (PBS)**, **PDA-**

P[5]OH@DOX, **PDA-P[5]OH-FA-Py@DOX**, at DOX equivalent dose of 6.5 mg/kg and **PDA-P[5]OH** dose of 21.0 mg/kg. As for the **PDA-P[5]OH-FA-Py@DOX +NIR** group, the tumor sites were irradiated with 808 nm NIR laser (1.0 W/cm², 5 min) at 12h post-injection. Every two days, the mice's body weight and tumor volume were assessed, and the tumor volume (V) is calculated according to the following equation: $V = 1/2 \times \text{length} \times \text{width}^2$. The tumor inhibitory rates (TIR) is calculated by the equation: $\text{TIR} (\%) = 100 \times (\text{mean tumor volume of the control group} - \text{mean tumor volume of others}) / (\text{mean tumor volume of the PBS group})$. At the end of the treatment, all tumors and major organs (heart, liver, spleens, lung, and kidneys) were dissected for histological examination by H&E staining and TUNEL assays.

2. Synthesis of P[5]OH

Scheme S1. Synthetic route to **P[5]OH**



By condensation of 1,4-dimethoxybenzene (DMB) (15.87 g, 0.115 mol) and methyl 2-(4-butoxyphenoxy)acetate (6.83 g, 0.03 mol) with para-formaldehyde and an

appropriate Lewis acid as a catalyst. **P1** was obtained after 4 h and purified by column chromatography (silica gel, PE : EA = 6 : 1), yield, 80 %.^{S1} **P2** (yield, 50 %) could be obtained by the reaction between **P1** (1g, 0.001 mol) and Ethylenediamine (1.335 mL, 0.02 mol) with ethanol as the solvent under refluxing for 12 h. Then, we successfully made use of **P2** (0.4 g, 0.5 mmol) and 3,4-Dihydroxyphenylaceticacid (0.08 g, 0.5 mmol) to synthesize Pillar[5]arene-OH (**P[5]OH**) (yield, 50 %) under the condition of 2-(7-Azabenzotriazol-1-yl)-*N,N,N',N'*-tetramethyluronium hexafluoro-phosphate (0.57 g, 1.5 mmol) and *N,N*-Diisopropylethylamine (0.26 g, 2 mmol).

P1: ¹H NMR (400 MHz, CDCl₃) δ 6.90 (s, 1H), 6.87 - 6.76 (m, 6H), 6.72 (d, *J* = 16.0 Hz, 2H), 6.63 (s, 1H), 4.45 (s, 2H), 3.88 (t, *J* = 6.0 Hz, 2H), 3.84-3.57 (m, 34H), 2.90 (s, 3H), 1.87-1.71 (m, 2H), 1.62-1.45 (m, 3H), 0.99 (m, 3H).

P2: ¹H NMR (400 MHz, CDCl₃) δ 6.95 (m, 6H), 6.79 (d, *J* = 12.0 Hz, 3H), 6.57 (s, 1H), 4.45 (s, 2H), 3.96 (t, *J* = 6.0 Hz, 3H), 3.92 - 3.62 (m, 34H), 1.94 - 1.76 (m, 2H), 1.59 (m, 2H), 1.02 (t, *J* = 16 Hz, 3H). ¹³C NMR (100 MHz, DMSO-*d*₆, 298K) δ (ppm): 167.3, 150.9, 150.5 (2C), 150.3, 150.2, 150.1, 150.0, 149.5, 148.4, 129.3, 128.5, 128.2, 128.0 (2C), 127.8, 127.7, 127.0, 126.5, 116.0, 114.3, 114.0, 113.9, 113.8, 113.7, 113.6, 113.4, 113.3, 113.2, 68.4, 67.1, 56.1, 55.9, 55.8, 55.7, 55.6, 41.5, 40.7, 31.6, 31.3, 30.0, 29.2, 28.8, 27.4, 19.4, 14.2; MS (*m/z*): HRMS (ESI) Calcd. For C₅₁H₆₃N₂O₁₁ ([M + H]⁺): 879.4426, found: 879.4447.

P[5]OH: ¹H NMR (400 MHz, DMSO-*d*₆) δ 9.45~9.35 (m, 2H), 8.14~8.05 (m, 2H), 6.85~6.76 (m, 13H), 4.31 (s, 2H), 3.86~3.83 (m, 2H), 3.77 (s, 2H), 3.66~3.64 (m, 30H), 3.27~3.22 (m, 2H), 3.01 (s, 2H), 2.89 (s, 2H), 1.70~1.68 (m, 2H), 1.49~1.47 (m, 2H), 1.21~1.16 (m, 2H), 0.93~0.91 (m, 3H). ¹³C NMR (100 MHz, DMSO-*d*₆): 208.42, 171.53, 153.00, 152.75, 152.71, 145.93, 145.86, 130.24, 129.94, 129.22, 129.14, 119.74, 118.71, 116.17, 114.95, 114.70, 112.79, 73.76, 69.67, 56.05, 54.37, 41.13,

31.64, 31.09, 24.16, 19.21, 13.78. MS (m/s): HRMS (ESI) Calcd. for $C_{59}H_{68}N_2O_{14}$ ($[M+Na]^+$): 1051.4567, found: 1051.4518.

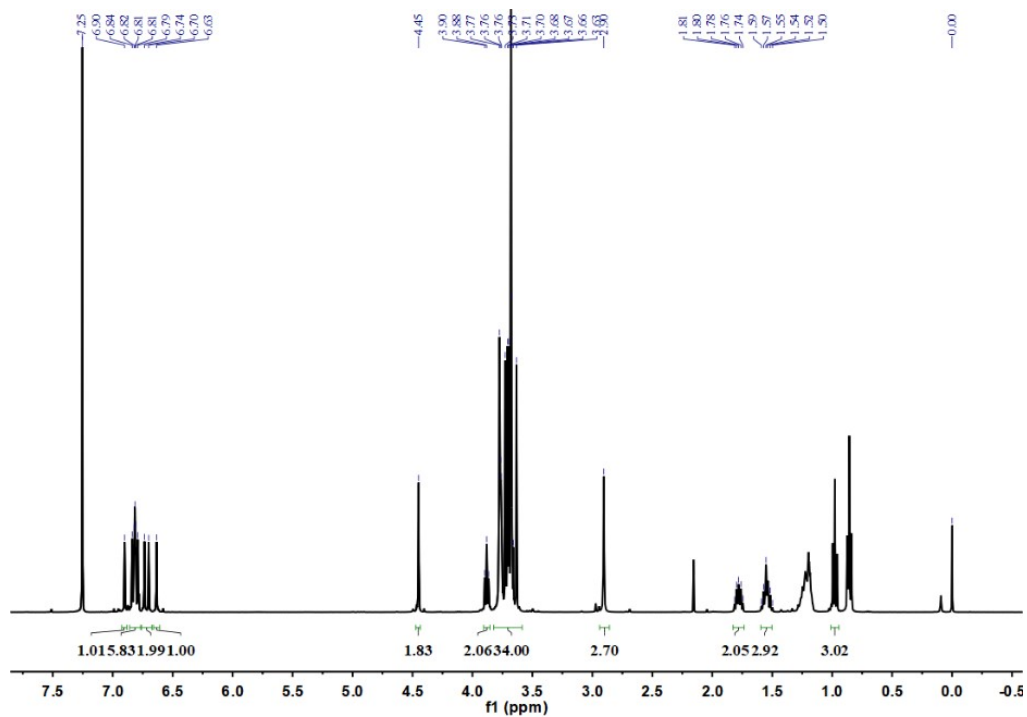


Figure S1. 1H NMR (400 MHz, 298K, $CDCl_3$) spectrum of P1.

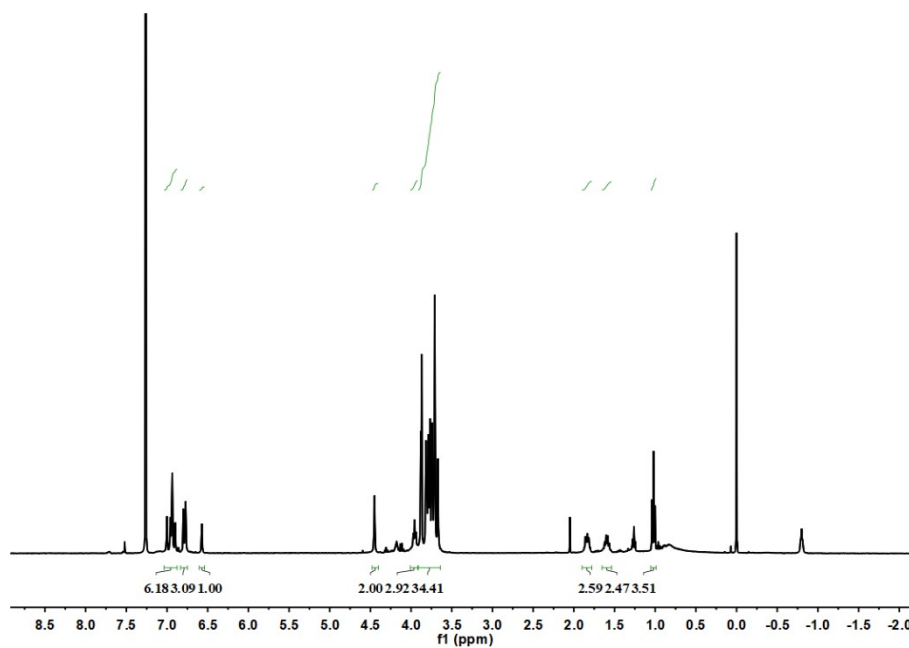


Figure S2a. 1H NMR (400 MHz, 298K, $CDCl_3$) spectrum of P2.

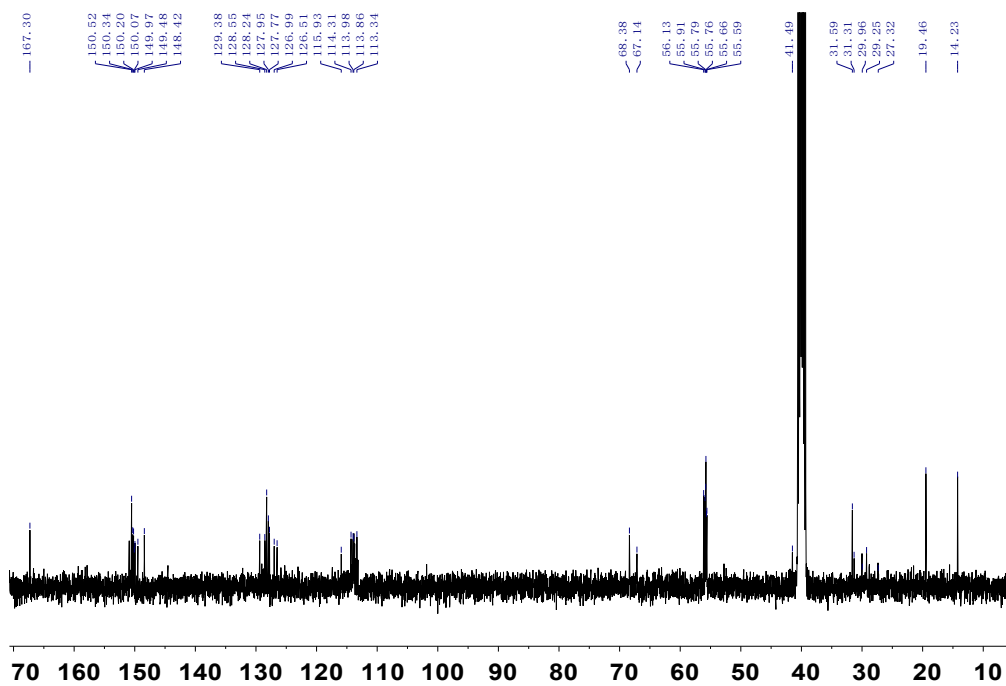


Figure S2b. ^{13}C NMR (100 MHz, $\text{DMSO-}d_6$, 298K) spectrum of **P2**.

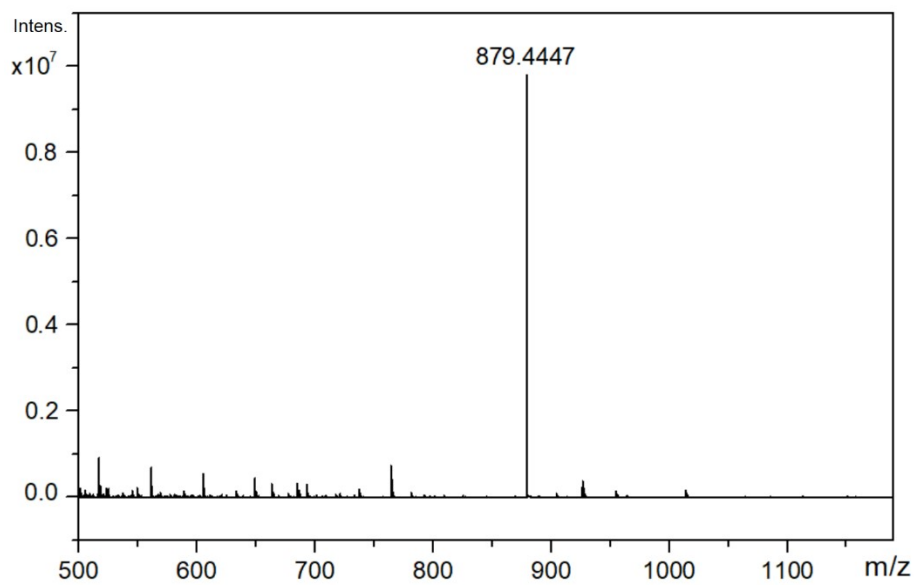


Figure 2c. HRMS spectrum of **P2**. Calcd. For $\text{C}_{51}\text{H}_{63}\text{N}_2\text{O}_{11}$ ($[\text{M} + \text{H}]^+$): 879.4426, found: 879.4447.

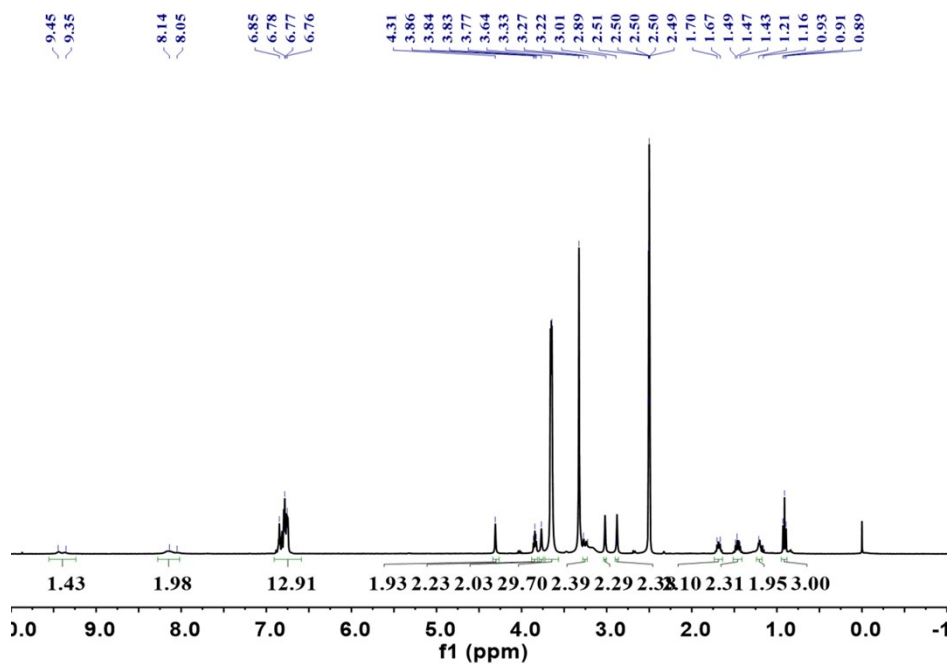


Figure S3. ^1H NMR spectrum (400 MHz, $\text{DMSO-}d_6$, 298K) of **P[5]OH**.

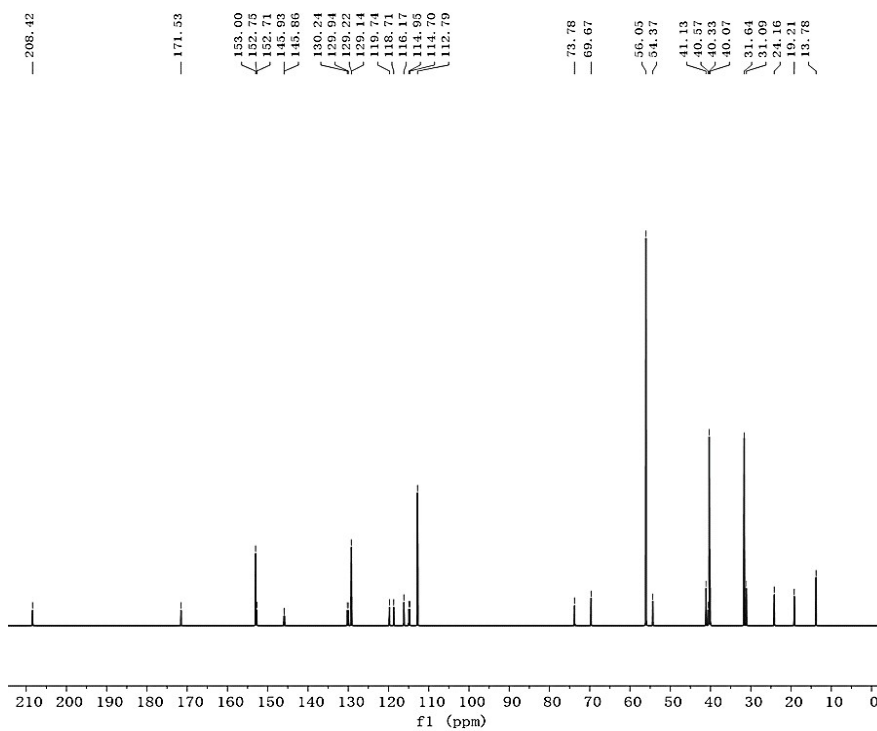


Figure S4. ^{13}C NMR spectrum (100 MHz, $\text{DMSO-}d_6$, 298K) of **P[5]OH**.

10 #13 RT: 0.20 AV: 1 NL: 3.10E7
T: FTMS + p ESI Full ms [100.0000-1500.0000]

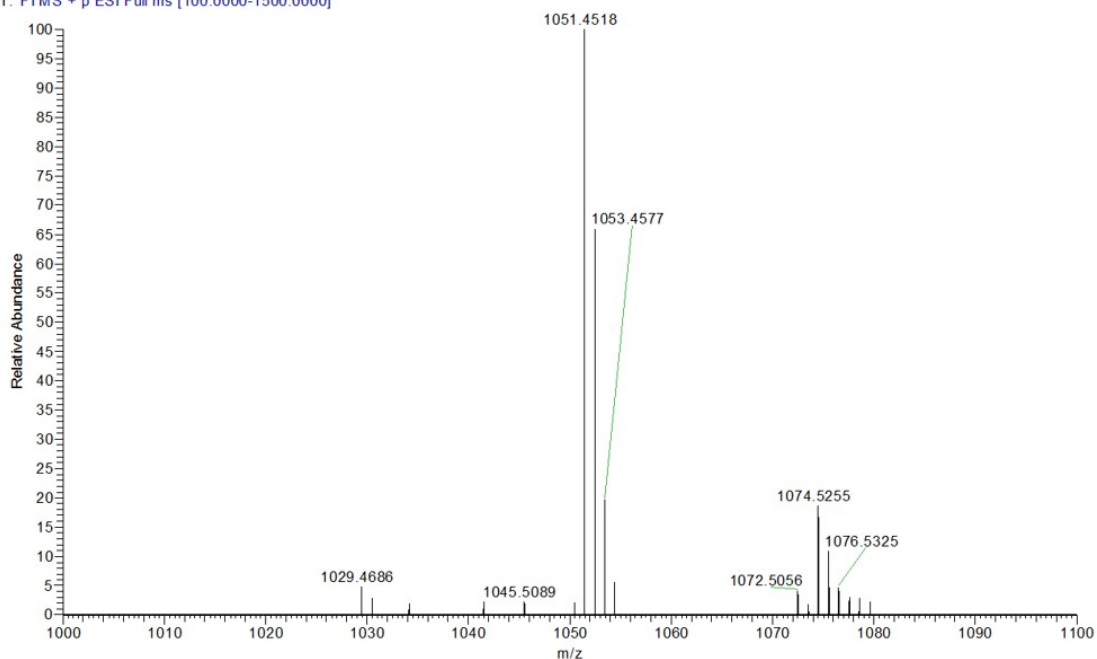


Figure S5. HR-MS (ESI) of **P[5]OH**. HRMS (ESI) Calcd. for $C_{59}H_{68}N_2O_{14}$ ($[M + Na]^+$): 1051.4567, found: 1051.4518.

3. Construction of PDA-P[5]OH nanoparticles

3.1 Synthesis of PDA-P[5]OH

Trometamol (0.41 g) was dissolved in 200 mL deionized water and stirred at 30 °C for half an hour. Then after adding dopamine hydrochloride (0.04 g) which was dissolved in 0.8 mL deionized water, Pillar[5]arene-OH (0.005 g) dissolved in 0.2 mL N,N-Dimethylformamide (DMF) was added dropwise in above solution. After stirring for 24h, the solution of **PDA-P[5]OH** was transferred into a dialysis bag (MWCO = 3500 Da) for 24 h. Finally, the **PDA-P[5]OH** nanoparticles were obtained by lyophilization.

3.2 Synthesis of PDA-P[5]OH-FA-Py

4 mg of **PDA-P[5]OH** was suspended in deionized water, then **FA-Py** (0.5 mg/mL) was added in **PDA-P[5]OH** solution. After stirring for 12 h, the solution of **PDA-P[5]OH** was transferred into a dialysis bag (MWCO = 3500 Da) for 24 h to obtain the **PDA-P[5]OH-FA-Py** solution.

3.3 Synthesis of PDA-P[5]OH-FA-Py@DOX

PDA-P[5]OH-FA-Py (2 mg) was dissolved in 2 mL of phosphate buffer saline (PBS, pH = 7.4), to which 2 mL of DOX·HCl (1 mg/mL) was added dropwise. After stirring for 24 h, the resulting solution was centrifuged and the free drug could be removed during this period. The absorption of DOX could be measured by UV-vis spectrometer at 480 nm, the DOX loading capacity can be calculated by UV-vis spectrum:

DOX loading capacity = (weight of initial DOX - weight of DOX in supernatant)/weight of PDA-P[5]OH-FA-Py = 317 $\mu\text{g}/\text{mg}$.

3.4 DOX release in vitro

The DOX release kinetics was detected by adding PDA-P[5]OH@DOX (2 mg) into different pH PBS solution (15 mL) with or without NIR (808 nm, 1.0 W cm^{-2}) irradiation. Then every one hour, the solution was measured the released DOX amount by UV-Vis spectroscopy.

The release of DOX was tracked using HPLC (Fig. S18). Due to the presence of the pillar[5]arene cavity, the PDA-P[5]OH NPs showed host-guest recognition capability (Fig. S8), and FA-Py as a target molecule was easily introduced into PDA-P[5]OH@DOX NPs to fabricate PDA-P[5]OH-FA-Py@DOX nanoparticles through the host-guest interaction. The obtained PDA-P[5]OH-FA-Py@DOX NPs were fully characterized using TEM (Fig. S14c), SEM (Fig. S14d), XPS (Fig. S17), and TGA analysis (Fig. S16).

4. Characterization

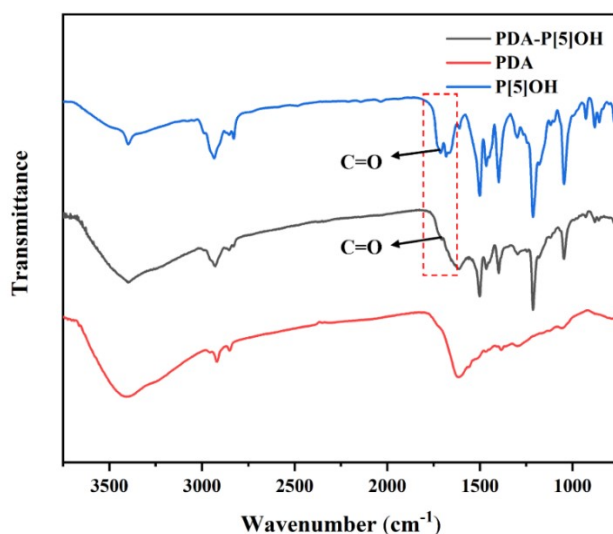


Figure S6. FR-IR spectra of PDA (red line), P[5]OH (blue line) and PDA-P[5]OH (black line).

In the FT-IR spectrum, the stretching vibration absorption of the C=O groups in **PDA-P[5]OH NPs** appeared at 1690 cm^{-1} , which is similar to that in **P[5]OH**, indicating that **P[5]OH** was successfully copolymerized with **DA**.

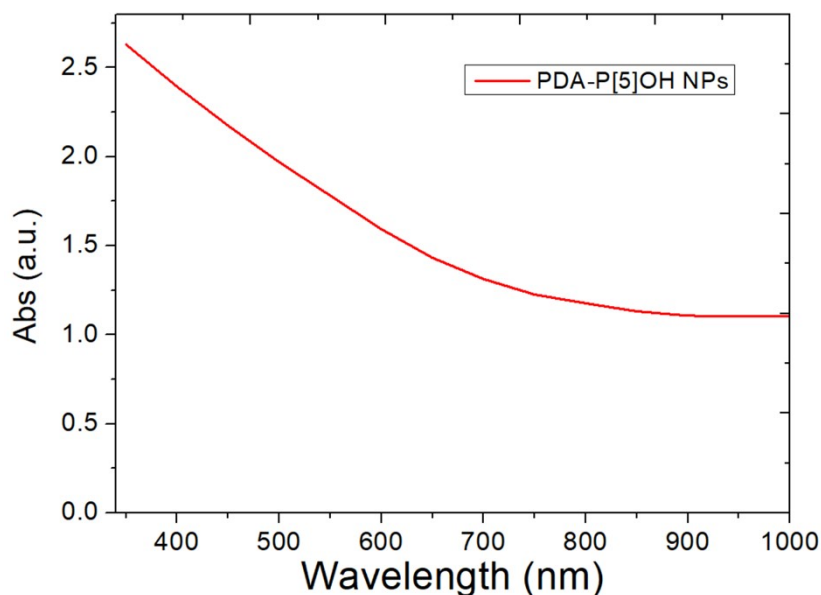


Figure S7. UV-Vis spectrum of **PDA-P[5]OH** nanoparticles.

Photothermal conversion efficiency:

When the concentration of **PDA-P[5]OH** nanoparticles was 2 mg/mL , the highest temperature is 42.3°C .

$$T_{\max} = 42.3^\circ\text{C} \quad T_{\text{sur}} = 20^\circ\text{C} \quad T_0 = 21^\circ\text{C}$$

$$h_s = \frac{m\text{CH}_2\text{O}}{\tau_s} = \frac{0.5 \times 4.2}{154.57} = 0.0136$$

$$Q_{\text{dis}} = \frac{cm\Delta T}{\Delta t} = \frac{0.5 \times 4.2 \times (42.3 - 21)}{480} = 0.09$$

$$y = \frac{0.0136 \times (42.3 - 20) - 0.09}{1 \times (1 - 10^{-0.95})} = 24.02\%$$

5. Host-guest interaction^{S2}

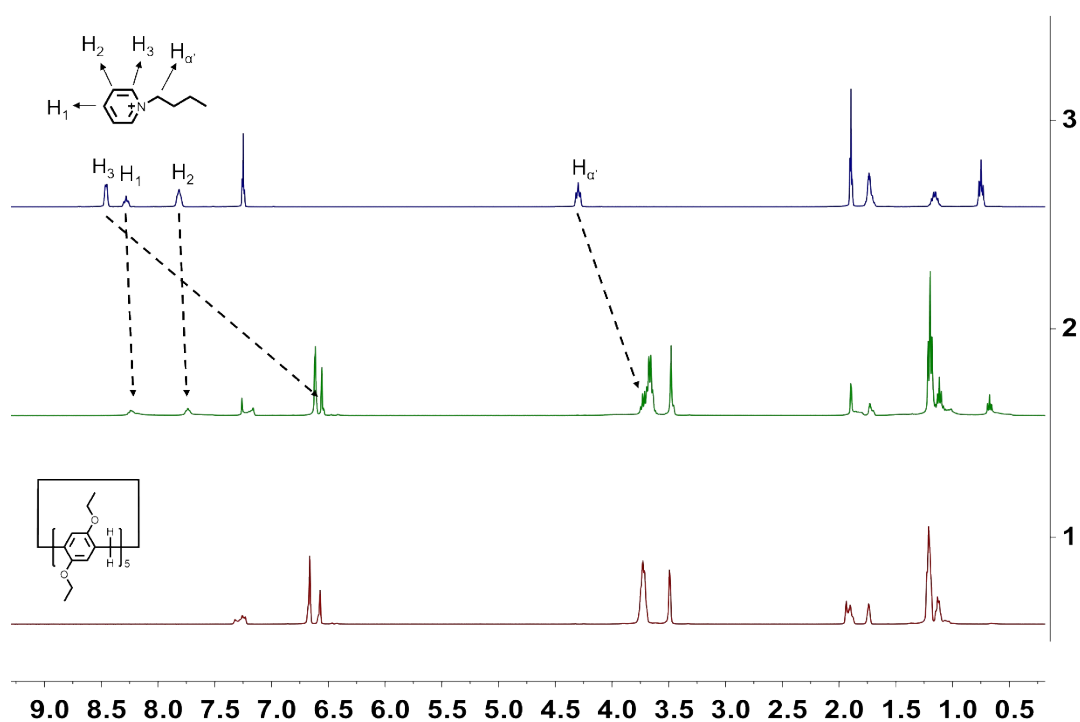


Figure S8. ¹H NMR spectra (400 MHz, CDCl₃/Acetonitrile-D₃, 298 K) of (1) pillar[5]arene (10.0 mM), (2) pillar[5]arene + model guest ([pillar[5]arene] = [model guest] = 10.0 mM), and (3) model guest (10.0 mM).

From ¹H NMR spectra, we confirmed that strong host-guest interaction exists between pillar[5]arene and the model guest.

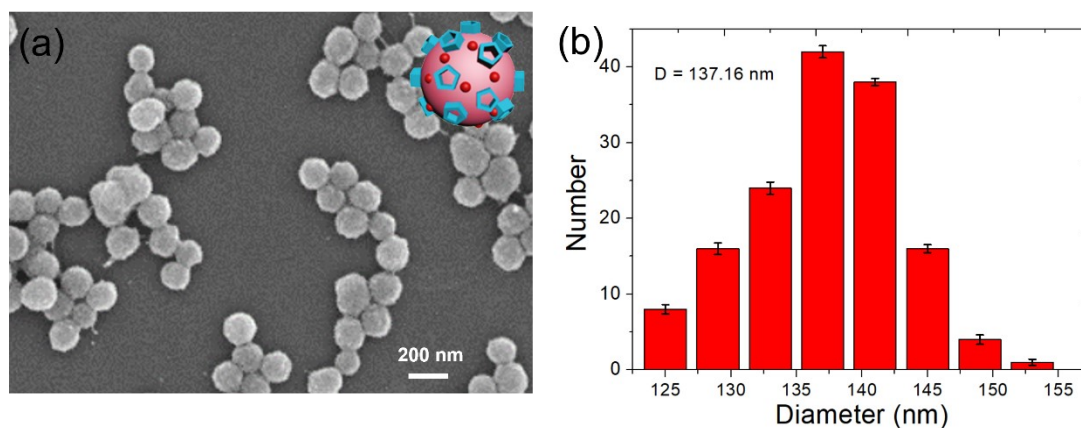


Figure S9. (a) SEM image and (b) size distribution of **PDA-P[5]OH@DOX** nanoparticles.

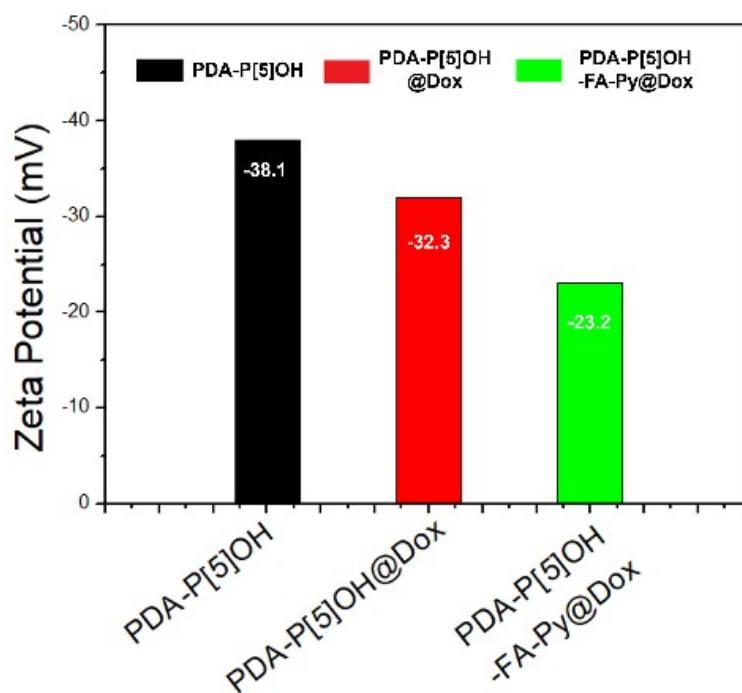


Figure S10. The zeta potential of **PDA-P[5]OH**, **PDA-P[5]OH@DOX**, and **PDA-P[5]OH-FA-Py@DOX**.

Zeta potential of **PDA-P[5]OH**, **PDA-P[5]OH@DOX**, and **PDA-P[5]OH-FA-Py@DOX** were -38.1 mV, -32.3 mV, and -23.2 mV, respectively.

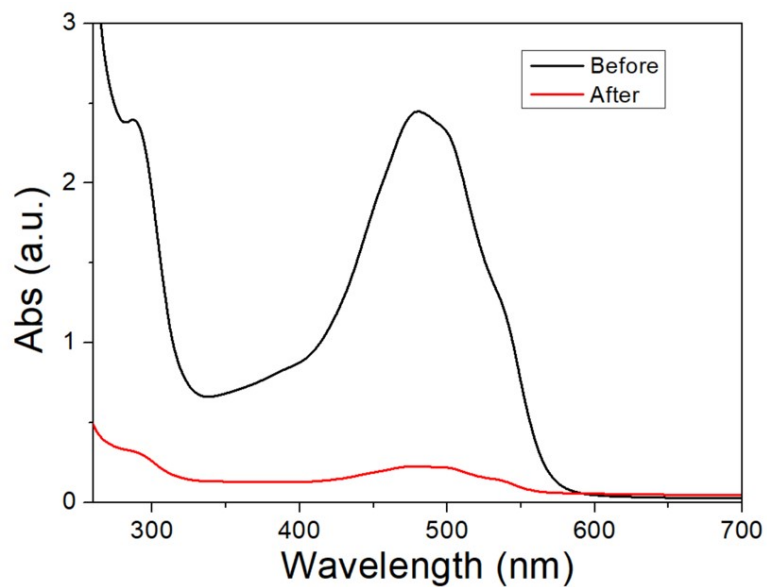


Figure S11. UV-vis spectra of DOX solution before and after adding of PDA-P[5]OH.

6. In vivo study

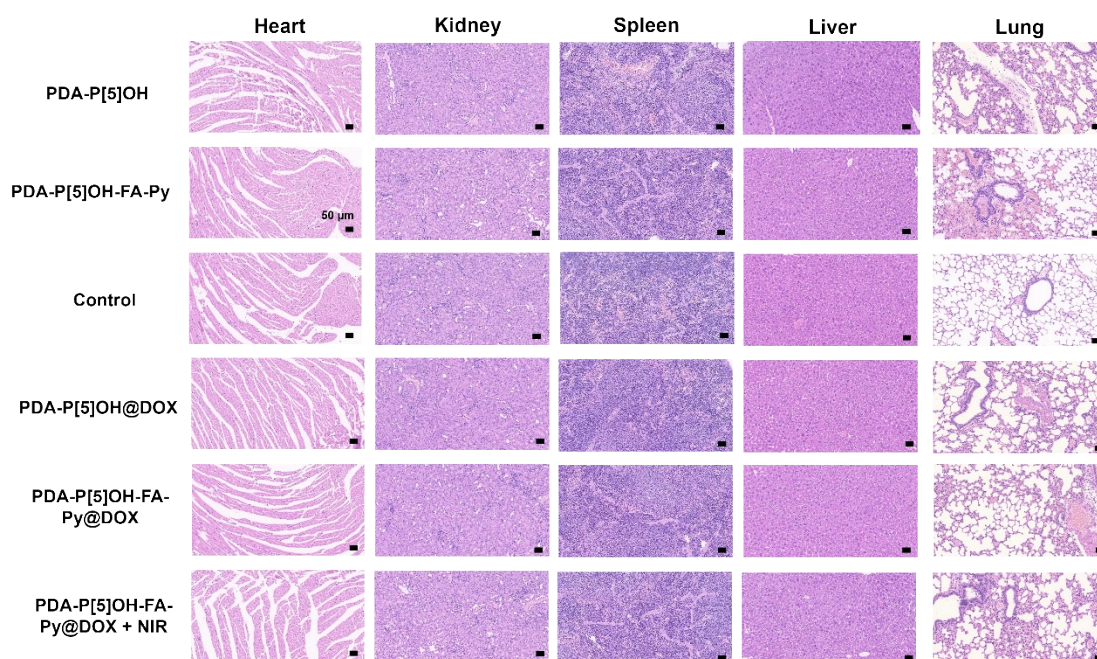


Figure S12. Representative H&E stained images of major organs collected from the mice with different treatment. Scale bar = 50 μ m.

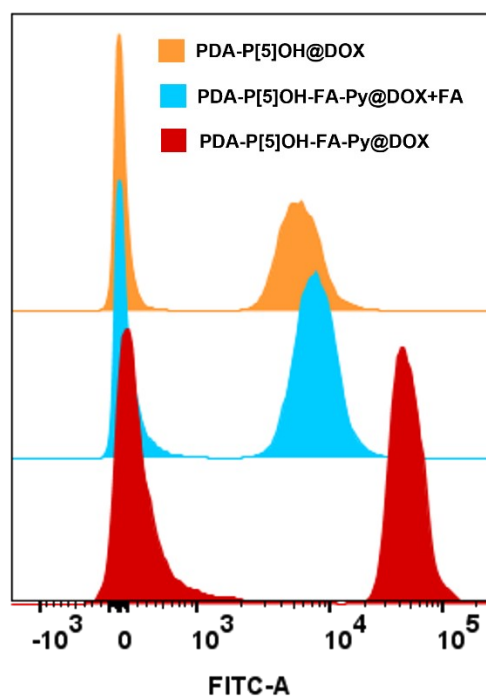


Figure S13. Flow cytometry histograms of **PDA-P[5]OH@DOX**, **PDA-P[5]OH-FA-Py@DOX**, and **PDA-P[5]OH-FA-Py@DOX + Free FA**.

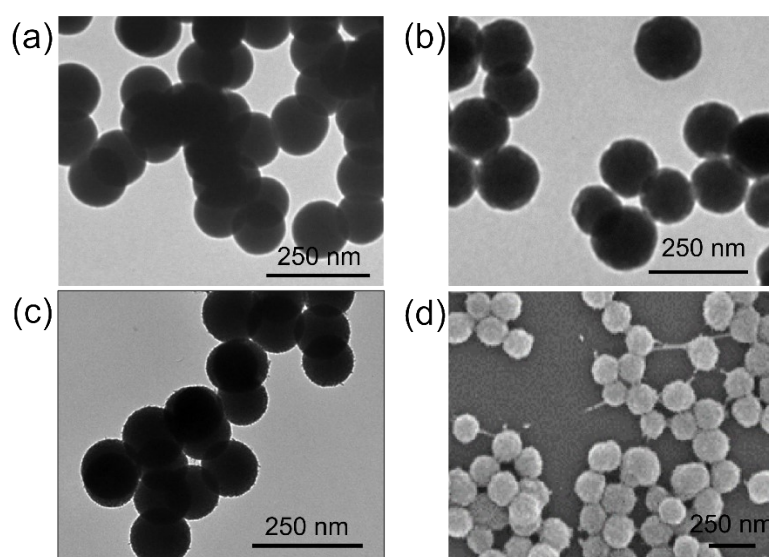


Figure S14. TEM images of (a) **PDA-P[5]OH NPs**, (b) **PDA-P[5]OH-FA-Py NPs** and (c) **PDA-P[5]OH-FA-Py@DOX NPs**. (d) SEM image of **PDA-P[5]OH-FA-Py@DOX NPs**.

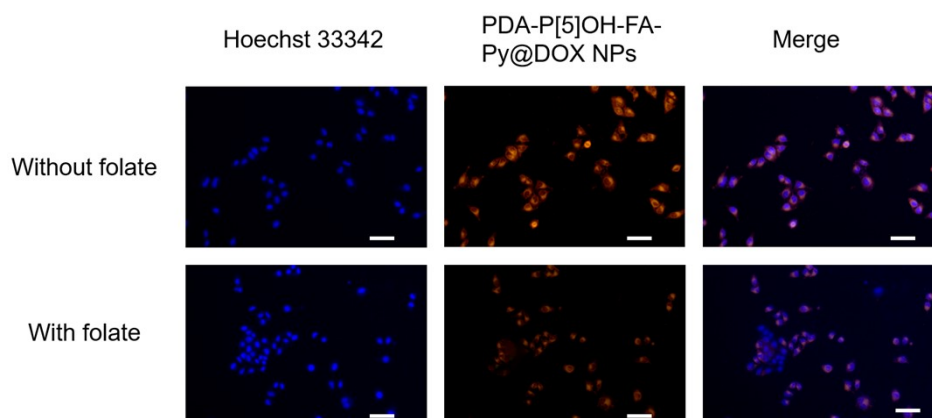


Figure S15. Fluorescence images of HeLa cells incubated with **PDA-P[5]OH-FA-Py@DOX** or **PDA-P[5]OH-FA-Py@DOX + Folate** for 1 h.

The cells treated with **PDA-P[5]OH-FA-Py@DOX** showed stronger fluorescence than did those treated with **PDA-P[5]OH@DOX** according to a quantitative flow cytometry analysis (Fig. S13). On the other hand, when HeLa cells were treated with **PDA-P[5]OH-FA-Py@DOX + folate**, the fluorescence intensity was decreased approximately 6.25-fold relative to that for the **PDA-P[5]OH-FA-Py@DOX** group (Fig. S13 and S15), due to free folate acting as a competitor to decrease the uptake of **PDA-P[5]OH-FA-Py@DOX** in HeLa cells. All the above results indicated the amazing targeting ability of **FA-Py** in **PDA-P[5]OH-FA-Py@DOX** particles.

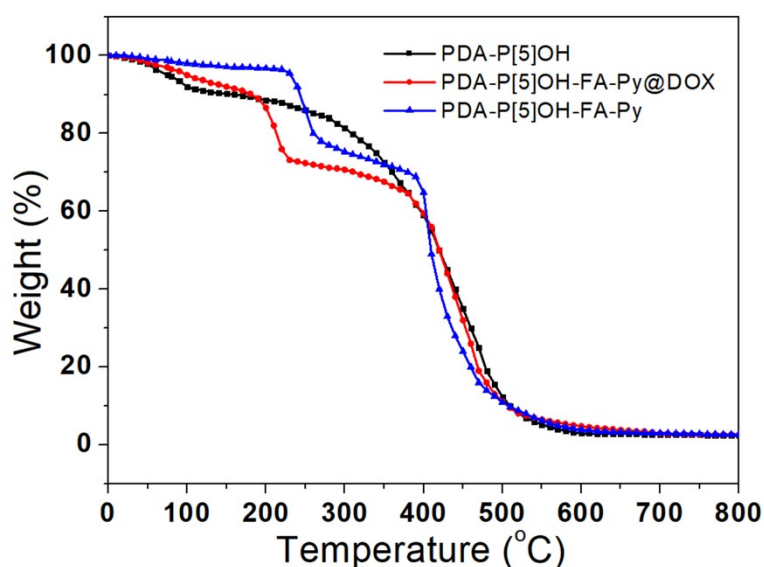


Figure S16. Thermogravimetric analysis (TGA) of **PDA-P[5]OH**, **PDA-P[5]OH-FA-Py@DOX**, and **PDA-P[5]OH-FA-Py** NPs.

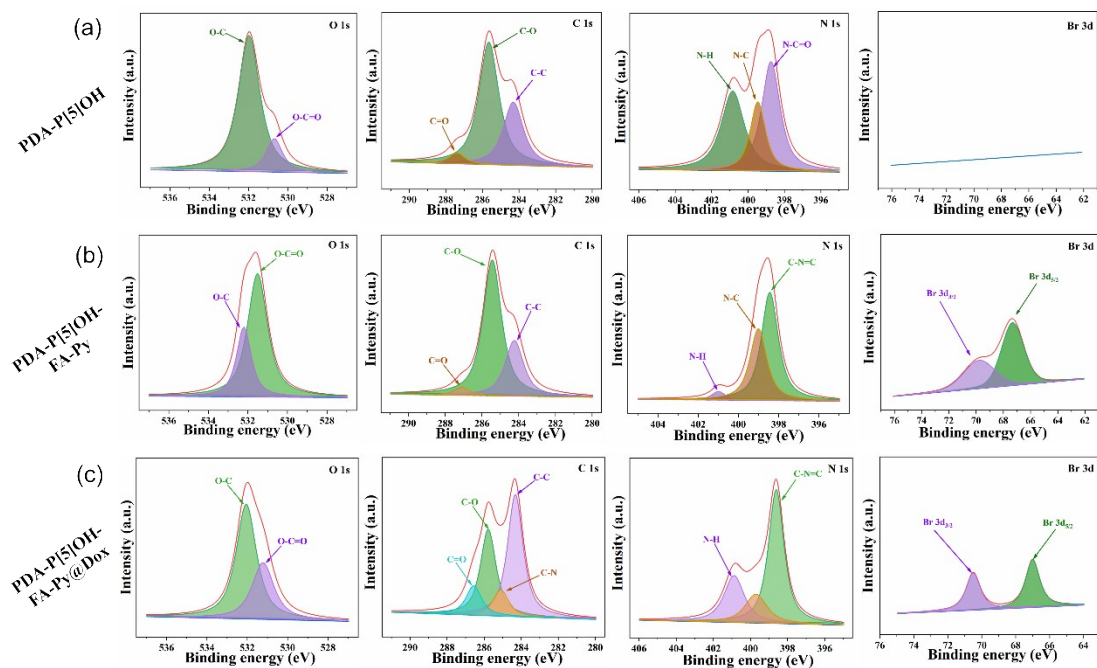


Figure S17. High-resolution XPS spectra of (a) PDA-P[5]OH, (b) PDA-P[5]OH-FA-Py, (c) PDA-P[5]OH-FA-Py@Dox.

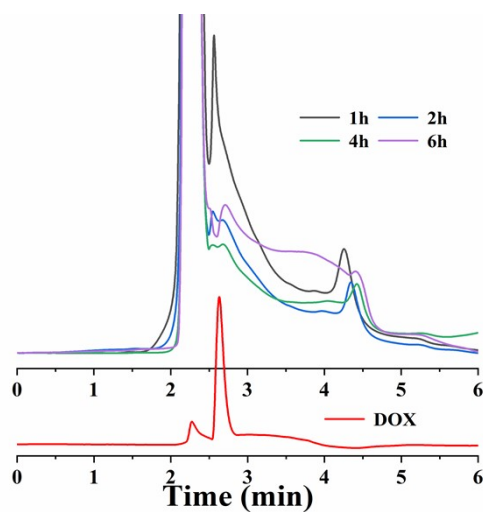


Figure S18. HPLC spectra of pure Dox solution and Dox release from PDA-P[5]OH-FA-Py@Dox with different time.

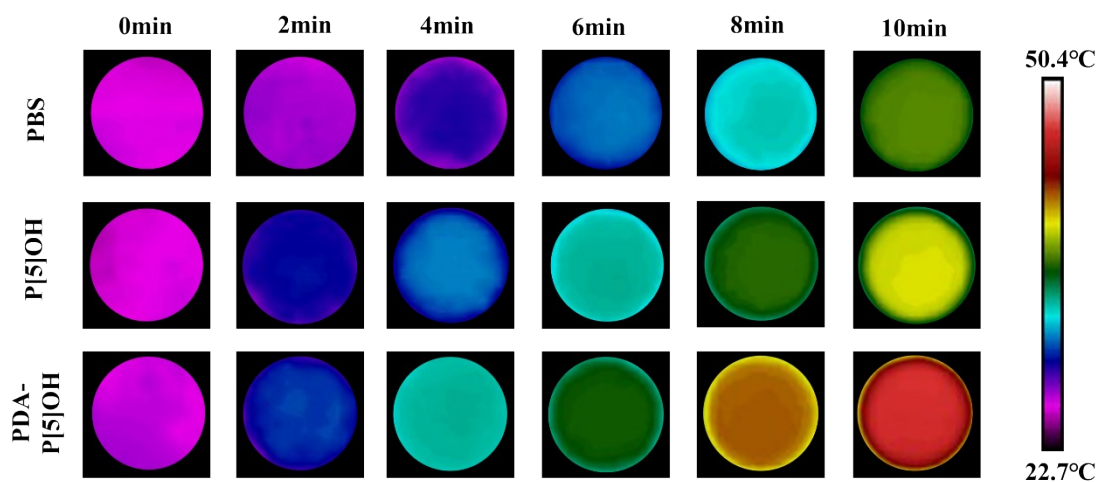


Figure S19. Photothermal images of **PBS** (control), **P[5]OH**, and **PDA-P[5]OH** NPs at 10 minutes of irradiation. (laser: 808-nm wavelength and 1.0 W cm^{-2}).

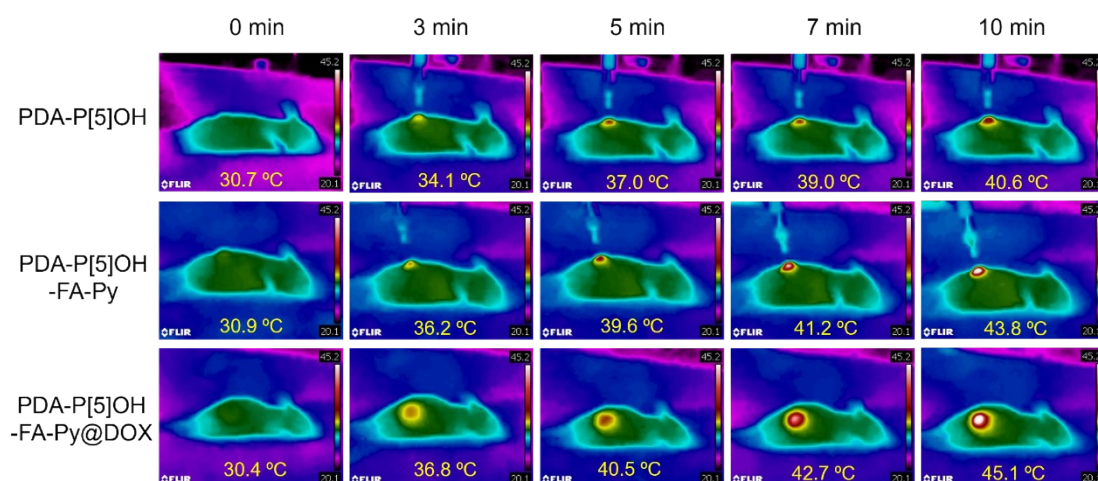


Figure S20. Photothermal images of mice subjected to indicated treatments over the indicated irradiation times.

As shown in Fig. S20, in the case of **PDA-P[5]OH**, a maximum temperature of only $38.7 \text{ }^\circ\text{C}$ was reached. In sharp contrast, the mice treated with **PDA-P[5]OH-FA-Py** and **PDA-P[5]OH-FA-Py@DOX** showed increases in temperature from 32.6 to 44.6 and $45.2 \text{ }^\circ\text{C}$, respectively. This mild photothermal effect has been shown to have a treatment effect on cancer without causing damage to the skin. This result further confirmed the excellent tumor targeting capacity of **FA-Py** in the particles.

References

S1. R. Zhang, X. Yan, H. Guo, L. Hu, C. Yan, Y. Wang, and Y. Yao, *Chem. Commun.*, 2020, **56**, 948-951.

S2. Y. Wang, D. Wang, J. Wang, C. Wang, J. Wang, Y. Ding and Y. Yao, *Chem. Commun.*, 2022, **58**, 1689-1692.